# Supporting Information

Jose et al. 10.1073/pnas.1210040109

## SI Text

**Further Details for Materials and Methods.** ***Protein purification and properties.*** The T4-coded DNA replication helicase (gp41) was cloned and overexpressed in *E. coli* OR1264/pDH518 cells (1) and purified as previously described (2). The T4 primase (gp61) protein carries a his-tag* and was prepared and purified as reported previously (3). The concentrations of purified gp41 and gp61 were determined by UV absorbance at 280 nm, using molar (per subunit) extinction coefficients ($\varepsilon_{M,280}$) of $7.6 \times 10^4$ $M^{-1}$-$cm^{-1}$ for gp41 and $6.9 \times 10^4$ $M^{-1}$-$cm^{-1}$ for gp61. These extinction coefficients were calculated from amino acid composition data as described elsewhere (4, 5).

***Further details on analytical ultracentrifugation procedures used.*** In each experiment 400 μl of sample and 410 μl of reference buffer were loaded, respectively, into the sample and reference sectors of a 1.2-cm double-sector Epon centerpiece in a standard analytical ultracentrifuge cell. In experiments involving GTPγS, equal concentrations of this component were added to both the reference and the sample sectors. Sedimentation velocity experiments were performed in a Beckman An60Ti ultracentrifuge rotor. Unless otherwise stated, experiments were run at 20 °C at a rotor speed of 50,000 rpm and monitored by UV absorbance at 280 nm. Sedimentation velocity data were collected continuously over periods of up to 8 h. The partial specific volume used in the sedimentation analysis, 0.735 ml/gm for gp41 and 0.74 ml/gm for gp61, were calculated based on the amino acid composition of the proteins. The buffer density (1.0076 gm/ml) measured with an Anton Paar densitometer and the viscosity (0.0103 Poise) was calculated using the SEDNTERP program (0.0103 Poise). All data analyses for the velocity sedimentation experiments were performed using the SedFit program (6–8). The root-mean-squared-deviations (rmsd) for all sedimentation velocity experiments were 0.008 or less. Sedimentation results were plotted as c (s) distribution plots of the relative concentrations of each size component versus $s_{20,w}$ (see Fig. S1).

**Other Supplementary Information.** ***T4 gp41 helicase hexamers alone do not form a stable complex with DNA.*** For optimal unwinding efficiency, a helicase should form a stable initiation complex with the replication fork DNA. We attempted to form such a helicase-DNA complex by adding gp41 to a solution of $dT_{45}$ oligomers (a run of T residues is the preferred loading site for gp41 on a DNA fork) in the presence of sufficient GTPγS to drive gp41 hexamer formation to completion. This mixture was subjected to sedimentation velocity analysis and the results showed only very weak association of the helicase with the DNA (Fig. S2*A*). In fact, while the smaller peak at approximately 11 S probably corresponds to gp41 hexamer bound to $dT_{45}$, the larger approximately 5.5 S peak likely corresponds to a dimer of gp41 bound to ssDNA, suggesting that $dT_{45}$ binding may partially destabilize the helicase hexamer.

Steady-state fluorescence anisotropy experiments were also performed in the presence of excess GTPγS to test the binding of the T4 gp41 hexamer helicase to ssDNA 5′ end labeled with Oregon Green dye (Table S1). Stable binding of the gp41 hexamers to ssDNA should result in an increase in the mass (and thus in the size and radius of gyration) of the complex, and this should be reflected as an increase in anisotropy of the protein-DNA complex with added gp41, followed by a plateau at binding saturation. The titration of gp41 into a solution containing 500 nM ssDNA and 60 μM GTPγS was plotted against gp41 concentration in Fig. S2*B* and only a very small increase in anisotropy with increasing gp41 concentration (and no plateau) were seen, suggesting, as expected from the ultracentrifuge results, that the gp41 helicase hexamer-DNA complexes formed under these conditions are very unstable.

***T4gp61 primase does not form defined complexes with ssDNA.*** To test potential order-of-addition assembly pathways for the T4 primosome, we mixed various concentrations of gp61 with ssDNA ($dT_{45}$) and subjected the resulting solutions to sedimentation velocity analysis. The results are shown as c(s) versus $s_{20,w}$ distribution plots in Fig. S3. Fig. S3*A* shows that gp61 primase alone sediments as a monomer in free solution, with $s_{20,w}$ = approximately 2.6 S. Fig. S3 *B* and *C* show c(s) versus $s_{20,w}$ plots for 1-μM and 1.5-μM solutions of gp61 (respectively) in the presence of 1.5 μM $dT_{45}$. The multiple peaks observed in these experiments suggest that primase subunits form relatively undefined aggregates with ssDNA, rather than defined complexes. The number and apparent $s_{20,w}$ values of the peaks increased with increasing gp61 concentration, suggesting that larger aggregates form with ssDNA at higher primase concentrations.

Steady-state fluorescence anisotropy experiments confirmed this interpretation of the sedimentation analysis. A stock gp61 solution containing GTPγS was titrated into a fixed concentration of 5′-OG-labeled ssDNA (see Table S1) and the observed change in anisotropy was plotted as a function of added gp61 (Fig. S3*D*). The resulting titration does not reach a plateau, even at very high primase concentrations. It is known that aggregation-induced light scattering can artificially increase apparent anisotropy values. Moreover, a decrease in apparent fluorescence intensity was observed at still higher ratios of gp61 to DNA, accompanied by the appearance of aggregates that were clearly visible to the naked eye. We conclude that T4 gp61 forms metastable aggregates with DNA in either the presence (fluorescence anisotropy) or the absence (ultracentrifugation) of GTPγS, and that initial mixing of T4 primase subunits with DNA prior to adding helicase results neither in the formation of defined DNA-primase complexes nor represents a viable pathway for assembling stable primosome-DNA complexes.

***Sedimentation velocity experiments with primase (gp61) subunit concentrations at less than stoichiometric (6:1) helicase:primase ratios.*** Fig. S6 demonstrates that the primosome complex is associating in 6:1 ratio in the presence of DNA. Note that the height of the gp41 c(s) peak at approximately 4.7 S is approximately constant in amount in all three runs (note different y-axes scales) suggesting that this may represent a fixed concentration of gp41 subunits that are damaged and incapable of assembly), while the height of the gp61 peak c(s) at 2.7 S increases with increasing primase subunit input. The equilibrium is obviously shifting towards primosome formation as the concentration of primase is increased, but the $s_{20,w}$ of the primosome component remains fixed at approximately 12.1 S, showing that larger oligomers are not formed in the presence of excess primase.

*We note that in most recent studies of the T4 replication system and its subassemblies (3, 9) the gp61 primase subunits used carried histidine tags at the N-terminal end to facilitate purification. We showed previously (3) that the unwinding and RNA priming activities of the his-tagged gp61 were increased approximately twofold over those of primase prepared without the his-tag, although all other properties of the primase preparations were the same.

1. Hinton DM, Silver LL, Nossal NG (1985) Bacteriophage T4 DNA replication protein 41. Cloning of the gene and purification of the expressed protein. *J Biol Chem* 260:12851–12857.
2. Dong F, Gogol EP, von Hippel PH (1995) The phage T4-coded DNA replication helicase (gp41) forms a hexamer upon activation by nucleoside triphosphate. *J Biol Chem* 270:7462–7473.
3. Jing DH, Dong F, Latham GJ, von Hippel PH (1999) Interactions of bacteriophage T4-coded primase (gp61) with the T4 replication helicase (gp41) and DNA in primosome formation. *J Biol Chem* 274:27287–27298.
4. Young MC, Kuhl SB, von Hippel PH (1994) Kinetic theory of ATP-driven translocases on one-dimensional polymer lattices. *J Mol Biol* 235:1436–1446.
5. Gill SC, von Hippel PH (1989) Calculation of protein extinction coefficients from amino acid sequence data. *Anal Biochem* 182:319–326.
6. Dam J, Schuck P (2005) Sedimentation velocity analysis of heterogeneous protein-protein interactions: Sedimentation coefficient distributions c(s) and asymptotic boundary profiles from Gilbert-Jenkins theory. *Biophys J* 89:651–666.
7. Dam J, Velikovsky CA, Mariuzza RA, Urbanke C, Schuck P (2005) Sedimentation velocity analysis of heterogeneous protein-protein interactions: Lamm equation modeling and sedimentation coefficient distributions c(s). *Biophys J* 89:619–634.
8. Schuck P (2000) Size-distribution analysis of macromolecules by sedimentation velocity ultracentrifugation and lamm equation modeling. *Biophys J* 78:1606–1619.
9. Valentine AM, Ishmael FT, Shier VK, Benkovic SJ (2001) A zinc ribbon protein in DNA replication: Primer synthesis and macromolecular interactions by the bacteriophage T4 primase. *Biochemistry* 40:15074–15085.


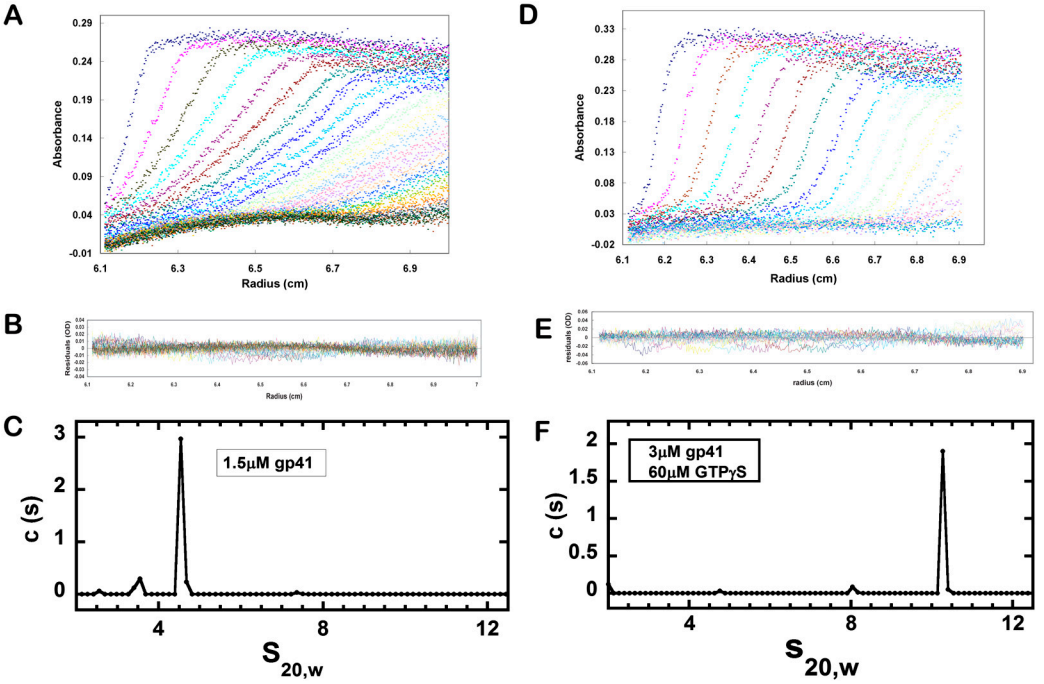


**Fig. S1.** Typical sedimentation velocity experiments with 3 μM gp41 at different input concentrations of GTPγS showing complete sedimentation profile and residual data sets as well as c(s) sedimentation distribution plots. (*A*) Sedimentation profiles; (*B*) residuals; and (*C*) c(s) sedimentation distribution plot for experiments performed at 3 μM gp41 subunit and 5 μM GTPγS concentrations. (*D*, *E*, and *F*) Equivalent plots for experiments performed at 3 μM gp41 subunit and 60-μM GTPγS concentrations. Experimental conditions and calculation procedures are described in *Materials and Methods* and *SI Text*.

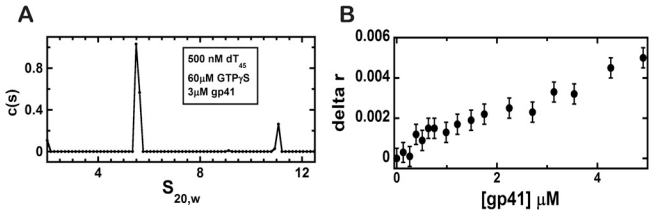


**Fig. S2.** Hexamers of gp41 assembled with GTPγS do not form stable complexes with ssDNA. (*A*) The c(s) versus $s_{20,w}$ distribution plot for a solution containing 500 nM $dT_{45}$, 60 μM GTPγS and 3 μM gp41 (subunits). The plot shows a large peak at approximately 5.5 S ($dT_{45}$-gp41 dimer complex?) and a smaller peak at approximately 11 S ($dT_{45}$-gp41 hexamer complex), suggesting that gp41-ssDNA complexes formed under these conditions are not stable. (*B*) Fluorescence anisotropy titration of gp41 with 5′-OG-ssDNA at 500 nM ssDNA and 60 μM GTPγS. Under these conditions we expect gp41 hexamer formation to be complete at approximately 3 μM gp41, but Fig. S2*B* shows no significant binding of the hexamer to ssDNA under these conditions.

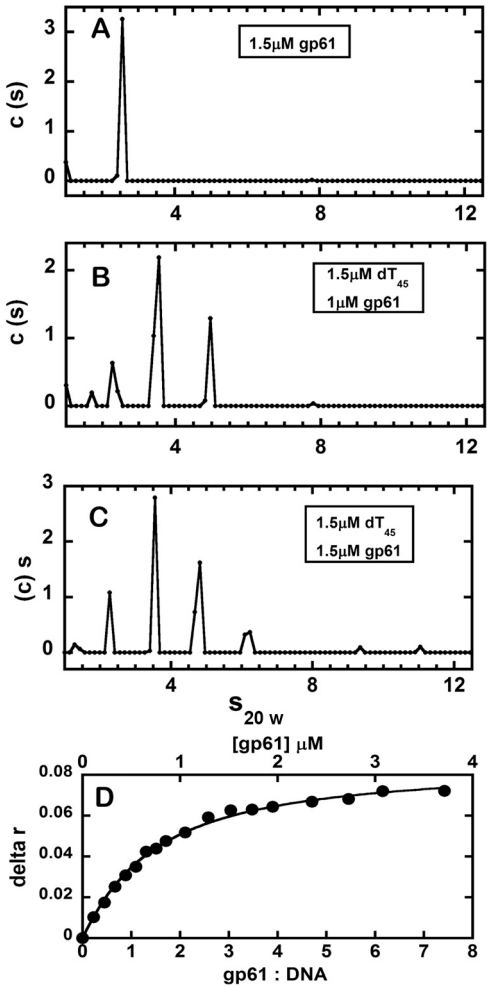


**Fig. S3.** *Sedimentation and fluorescence anisotropy experiments with T4 primase (gp61) subunits alone and with ssDNA in the absence and presence of GTPγS.* Sedimentation velocity c(s) distribution plots for: (*A*) 1.5 μM gp61 alone; (*B*) 1.5 μM $dT_{45}$ and 1 μM gp61; and (*C*) 1.5 μM $dT_{45}$ and 1.5 μM gp61. These solutions contained no GTP or GTPγS. The (c)s versus $s_{20,w}$ distribution plots showed a single peak at $s_{20,w} = 2.6$ S for gp61 monomer alone and a series of additional peaks for the solutions containing ssDNA. The number and $s_{20,w}$ values of these peaks increased with increasing gp61 concentration, suggesting the formation of undefined ssDNA-primase aggregates. (*D*) Steady-state fluorescence anisotropy experiments monitoring the titration of gp61 into a 500 nM solution containing 5′-Oregon green-labeled ssDNA and 60 μM GTPγS. The x-axis plots the molar ratio of gp61 subunits to DNA molecules. No plateau was reached, consistent with the formation of undefined primase-DNA aggregates.

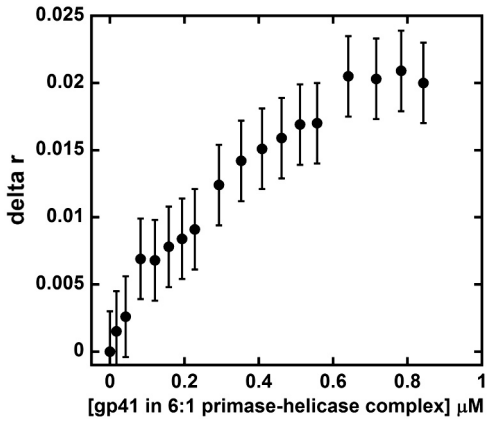


**Fig. S4.** Steady state fluorescence anisotropy experiments show that binding of preformed helicase-primase complex to DNA does not form a stable complex. Fluorescence anisotropy was used to monitor the titration of a premixed gp41-GTPγS-gp61 complex (same concentrations as in Fig. S3) titrated against 5′-end-labeled Oregon green ssDNA did not show a significant change in anisotropy, consistent with the results obtained with analytical ultracentrifugation that showed aggregation of initial pre-formed gp41-GTPγS-gp61 complexes when added to ssDNA.

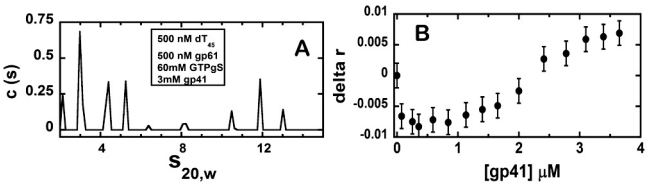


**Fig. S5.** Sedimentation velocity analytical ultracentrifugation and steady state fluorescence anisotropy experiments show that the order-of-addition of the individual components controls whether stable DNA-primosome complexes or undefined aggregates are formed. (*A*) A solution containing 500 nM concentrations of gp61 subunits was added to a 500 nM concentration of ss DNA construct, followed by the addition of 60 μM GTPγS and 3 μM gp41. A series of peaks was observed, indicating the formation of undefined DNA-protein aggregates. (*B*) Titration of gp41 into a solution containing 500 nM 5′-end-labeled Oregon green ssDNA, 60 μM GTPγS and 500 nM gp61 and monitored by fluorescence anisotropy shows that the complex initially formed between DNA and gp61 represents an aggregated state and that the addition of gp41 increased this aggregation.

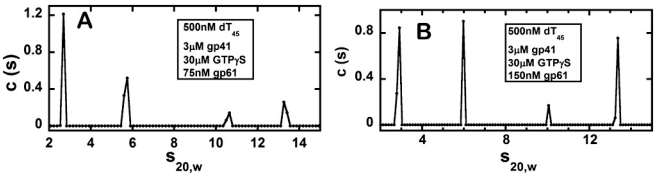


**Fig. S6.** Sedimentation velocity experiments with primase (gp61) subunit concentrations at less than stoichiometric (6:1) helicase:primase ratios. Sedimentation velocity c(s) distribution plots obtained with solutions containing: (*A*) 500 nM $dT_{45}$, 3 μM gp41, 30 μM GTPγS and 75 nM gp61 (a 40:1 ratio of gp41:gp61 monomers); and (*B*) 500 nM $dT_{45}$, 3 μM gp41, 30 μM GTPγS and 150 nM gp61 (a 20:1 ratio of gp41:gp61 subunits). The peaks at ∼13 S correspond to gp41 hexamers bound to a ssDNA construct and complexed with a single primase subunit (6:1 helicase-primase subunit complexes), while the peaks at approximately 10.5 S correspond to free gp41 hexamers and the peaks at $s_{20,w}$ to smaller gp41 assembly intermediates.

**A**

| | complex | $S_{20w}$ (calculated) | $S_{20w}$ (experimentally measured) |
|---|---|---|---|
| Gp41 monomer |  | 5.0S | 4.5S |
| gp41 dimer |  | 6.75S (26%) | ~6S (25%) |
| gp41 trimer |  | 8.21S (39%) | – |
| gp41 tetramer |  | 9.50S (47%) | ~8.2S (47%) |
| gp41 pentamer |  | 10.8S (54%) | – |

**B**

| | Complex | $S_{20,w}$ (Calculated by cubic substitution method*) | $S_{20,w}$ (Experimentally measured) |
|---|---|---|---|
| gp41 hexamer |  | 12.4S | 10.5S |
| gp41:gp61 (6:1 subunit ratio) |  | 13.1S (5%) | 12.1S (13%) |
| gp41:gp61 (6:1 subunit ratio) |  | 13.8S (10%) | 12.1S (13%) |
| gp41:gp61 (6:2 subunit ratio) |  | 14.1S (12%) | 12.1S (13%) |
| gp41:gp61 (6:3 subunit ratio) |  | 14.6S (15%) | 12.1S (13%) |
| gp41:gp61 (6:6 subunit ratio) | 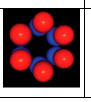 | 17.1S (28%) | 12.1S (13%) |

**Fig. S7.** (*A*) Hydrodynamic modeling of gp41 oligomers. The calculated $s_{20,w}$ values in column 3 were obtained using the cubic substitution method described in Carrasco et al. (1), which is currently considered the most reliable method for making such estimates. The experimentally determined values of $s_{20,w}$ for the gp41 oligomers assumed in the modeling to be present in each case are shown in column 4. The percentage values shown in column 3 represent the relative change in sedimentation coefficients taken against the calculated $s_{20,w}$ value of a non-hydrated sphere of molecular weight 55,000 Daltons in water at 20 °C. The percentage values in column 4 represents the change in sedimentation coefficients relative to the experimentally determined $s_{20,w}$ value of the gp41 monomer. The results suggest that the assignment of the two intermediate peaks of Fig. 2 to gp41 dimers and tetramers is very likely correct. (*B*) Hydrodynamic modeling of gp41 helicase and primase complexes. The calculated $S_{20,w}$ values in column 3(*) were obtained using the cubic substitution method described in Carrasco et al. (1), which is currently considered the most reliable method for making such estimates. Models of the primosome complex are shown in column 2. The resulting predicted $s_{20,w}$ values are shown in column 3(*). The percentage values represent the change in $s_{20,w}$ values relative to the predicted $s_{20,w}$ of the model gp41 hexamer. The experimentally determined $s_{20,w}$ values for the primosome complex are shown in column 4. The percentage values in column 4 (13% in all cases) represent the change of $s_{20,w}$ relative to the experimentally determined $s_{20,w}$ value of the gp41 hexamer. Comparison of the percentages in columns 3 and 4 suggest that these calculations can be used to rule out unambiguously only primosome structures containing more than 3 primase subunits per hexamer.

1 Carrasco B, Garcia de la Torre J (1999) Hydrodynamic properties of rigid particles: Comparison of different modeling and computational procedures. *Biophys J* 76:3044–3057.

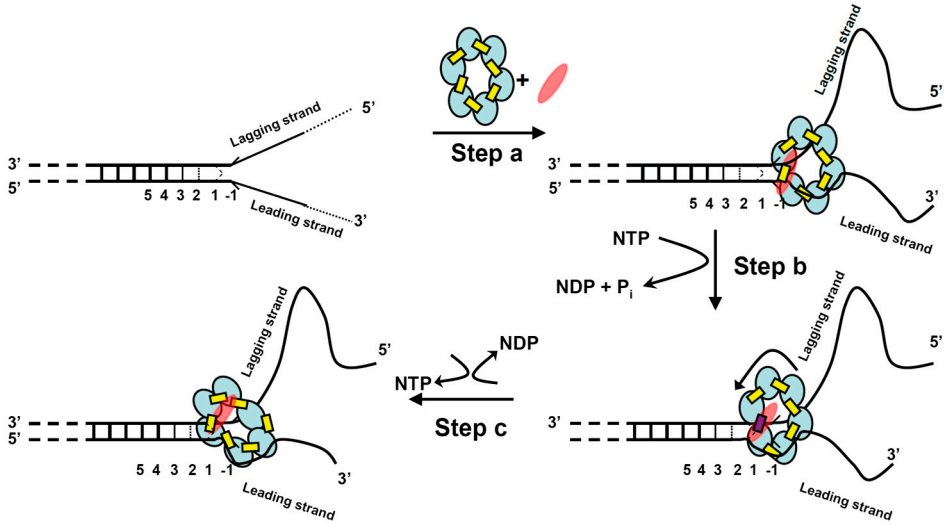


**Fig. S8.** A simple model for the unwinding of a replication fork by the T4 primosome helicase. The constituents of the primosome are shown as follows: gp41 subunits (blue ellipses), gp61 subunit (red ellipse), GTP (yellow rectangles), and GDP (red rectangle). The "degrees of openness" of the base pairs adjacent to the ss-dsDNA junction are obtained from earlier results (1) and the numbers below each DNA construct represent the numbering of the various bps of the DNA fork prior to initial helicase binding. Step (a). The GTP-bound gp41 hexameric helicase loads onto the free DNA fork construct and the gp61 primase subunit binds and stabilizes the complex at the fork junction. Positioning is facilitated by the uniquely unstacked conformation of the −1 bases. Step (b). GTP hydrolysis occurs at the gp41-gp41 interface positioned adjacent to the bound gp61 primase subunit, and the gp41 hexamer rotates by one subunit (approximately 60°) and the primase translocates to the next gp41-gp41 interface. Step (c). The GDP (and $P_i$) hydrolysis products formed in Step (b) dissociate, a new GTP binds and stabilizes the previously destabilized gp41-gp41 subunit interface, and the primosome helicase is ready to begin a new unwinding-rotation-hydrolysis cycle.

1 Jose D, Datta K, Johnson NP, von Hippel PH (2009) Spectroscopic studies of position-specific DNA "breathing" fluctuations at replication forks and primer-template junctions. *Proc Natl Acad Sci USA* 106:4231–4236.

**Table S1. Sequences of the DNA constructs used. Note that these constructs were also used in our spectroscopic study (DJ, SEW and PHvH, manuscript under review) using 2-AP base analogue probes site-specifically substituted for adenine (the probe positions are designated with red X's). 5′-OG designates the Oregon Green adduct positioned at the 5′-end of the ssDNA sequence. Both 5′-OG and 2-AP were used as fluorescence labels in the anisotropy titrations (see *Materials and Methods*)**

| Construct | DNA Sequence |
|---|---|
| **$dT_{45}$** | **5′−dT$_{22}$−dG−dT$_{22}$−3′** |
| **2-AP labeled ss DNA** | 5′TTTTTTTTTTTTTTTTTTTTTTTTTTTTTTTTGCACCATATA**X**TCGCTCGCATATTATGACTG |
| **5′-OG end-labeled ss DNA** | 5′OG-TTTTTTTTTTTTTTTTTTTTTTTTTTTTTTGCACCATATAATCGCTCGCATATTATGACTG |
| **2-AP monomer-labeled forked DNA construct** | 5′TTTTTTTTTTTTTTTTTTTTTTTTTTTTTTGCACC**ATATA**X**TCGCTCGCATATTATGACTG**<br>\|\|\|\|\|\|\|\|\|\|\|\|\|\|\|\|\|\|\|\|\|\|\|\|\|\|<br>3′CATTCGTGCACTCACTTTCACCATTTTCGTAG**TATATTAGCGAGCGTATAATACTGAC** |
| **2-AP dimmer-labeled forked DNAconstruct** | 5′TTTTTTTTTTTTTTTTTTTTTTTTTTTTTTGCACC**ATAT**XX**TCGCTCGCATATTATGACTG**<br>\|\|\|\|\|\|\|\|\|\|\|\|\|\|\|\|\|\|\|\|\|\|\|\|\|\|<br>3′CATTCGTGCACTCACTTTCACCATTTTCGTAG**TATATTAGCGAGCGTATAATACTGAC** |
| **ssDNA used in RNA priming aasay** | 5′-ACTGGCCGTTTTGTTCTGGATGA**GTTGGTTG**GACGGCTGCGAGGCTGCGG-3′ |